INCREMENTAL FORMING OF PERFORATED STAINLESS STEEL SHEETS

A thesis submitted in partial fulfilment
of the requirements for the award of the degree of

Bachelor of Technology

In

Mechanical Engineering

Submitted by
Veeranala Varshitha Preetham

22ME01028

Under the Supervision of
Dr. Gaurav Bartarya

School of Mechanical Sciences
Indian Institute of Technology Bhubaneswar
Argul, Jatni, Bhubaneswar - 752050

December, 2025

Incremental Forming of Perforated SS sheets

Abstract:

This project presents a detailed finite element simulation study on the incremental sheet forming (ISF) of perforated SS304L stainless-steel sheets using Abaqus CAE, as preparation for future experimental work. ISF is a flexible forming process commonly used to create complex shapes without the need for dedicated dies, making it suitable for low-volume and customized manufacturing. However, forming perforated sheets is more challenging because the presence of holes leads to stress concentration, uneven deformation, and a higher possibility of thinning. To understand how different process parameters influence the behaviour of perforated sheets during ISF, a systematic simulation approach was followed. Three main parameters were investigated: feed rate, step depth, and tool rotational speed. While changing the feed rate (600, 800, 1000 mm/min), the step depth and tool speed were kept constant at 0.2 mm and 300 rpm. While changing the step depth (0.1, 0.2, 0.3 mm), the feed rate and tool speed were fixed at 800 mm/min and 300 rpm. While changing the tool speed (200, 300, 400 rpm), the feed rate and step depth remained constant at 800 mm/min and 0.2 mm. These fixed values—800 mm/min feed, 300 rpm tool speed, and 0.2 mm step depth—were selected based on optimal conditions reported in literature. For each parameter combination, the forming response was assessed using contact forces, thickness variation, and . These results help explain how the sheet reacts under different forming conditions and how changing a single parameter affects stress levels, strain behaviour, and thickness reduction around the perforations. Overall, the study provides a clear comparison of forming performance under various ISF settings and offers useful guidance for selecting suitable process parameters. The findings also form a strong foundation for planning the upcoming experimental phase and for improving understanding of ISF behaviour in perforated stainless-steel sheets.

Keywords:

- Incremental Sheet Forming
- Step Depth
- Von Mises Stress
- Contact Force Analysis
- Deformation Behaviour

CONTENTS

LIST OF FIGURES

Fig. No.: Caption Page No.

LIST OF TABLES

CHAPTER 1:

INTRODUCTION

1.1 Theoretical Background

1.1.1 Incremental Sheet Forming (ISF)

Incremental Sheet Forming (ISF) is an advanced and flexible sheet metal forming process that enables the production of complex three-dimensional geometries without the requirement for dedicated dies or molds. It is categorized as a die-less forming technique and represents a modern alternative to traditional sheet metal forming methods such as deep drawing, stamping, and hydroforming, which rely on expensive and time-consuming tooling. The core concept of ISF lies in the localized plastic deformation of the sheet metal by a small, rounded forming tool that moves along a predetermined toolpath generated from a CAD model of the target geometry.

In the ISF process, a thin sheet metal blank is securely clamped along its periphery to restrict unwanted movement. A forming tool, generally possessing a hemispherical or conical tip, is mounted on a CNC machine or robotic arm. The tool follows a programmed trajectory while gradually descending in small vertical increments, thereby deforming the sheet locally at each pass. The accumulation of these localized deformations progressively shapes the sheet into the desired three-dimensional form.

ISF primarily depends on incremental deformation rather than uniform global deformation, leading to high strain localization near the contact zone between the tool and sheet. This localized nature of plastic flow allows the formation of intricate geometries through successive tool passes, with deformation occurring layer by layer. The material in the contact zone experiences combined stretching and bending stresses, while adjacent regions remain largely undeformed.

Based on tooling configuration, ISF is generally classified into two main categories:

1. Single Point Incremental Forming (SPIF): In SPIF, the forming is carried out using a single tool without any supporting die. The tool follows a spiral or contour-based toolpath, deforming the sheet progressively. This method provides simplicity in setup and flexibility in shape formation.

2. Two Point Incremental Forming (TPIF): In TPIF, an additional backing or supporting die is introduced beneath the sheet. This configuration improves geometric accuracy and dimensional control. The supporting structure can be partial, flexible, or solid, depending on the precision and complexity required.

The main process parameters influencing ISF include tool diameter, step size, feed rate, spindle speed, sheet thickness, material properties, and toolpath strategy. These parameters govern the final surface quality, thickness distribution, strain hardening, and dimensional accuracy of the formed component.

Mechanically, ISF involves localized plastic deformation in which only a small portion of the sheet is deformed at a time. The deformation zone moves progressively with the tool, resulting in non-uniform strain distribution through the sheet thickness. Although the process offers enhanced formability, challenges such as thickness reduction, spring-back, and dimensional inaccuracies remain important considerations.

Recent advancements in ISF research focus on toolpath optimization, process simulation, hybrid forming approaches, and temperature-assisted forming techniques to improve accuracy, predictability, and surface finish. The integration of ISF with digital manufacturing technologies and computer-aided process control has further improved its adaptability and precision.

1.1.2 Working Principle

The working principle of Incremental Sheet Forming (ISF) is based on the gradual and localized plastic deformation of a clamped sheet metal blank using a CNC-controlled forming tool. The tool, equipped with a smooth hemispherical tip, moves along a programmed path corresponding to the desired part geometry. Instead of deforming the entire sheet at once, the tool applies force on a small, localized region, producing plastic deformation only in that area.

As the tool moves incrementally along successive contours at different depths, these localized deformations accumulate, and the sheet gradually forms into the required three-dimensional shape. The vertical motion of the tool is controlled in small depth increments known as step size (Δz), which defines the layer thickness of each deformation pass. The movement of the tool in all three directions (X, Y, and Z) is precisely controlled by a CNC system to ensure accurate reproduction of the CAD model geometry.

During the ISF process, the sheet metal is subjected to a complex tri-axial stress state, which primarily includes the following:

1. Tangential (Hoop) Stress ($\sigma\theta$) – Tensile: This stress acts circumferentially around the tool contact zone. It is tensile in nature, as the material stretches to conform to the tool's motion around the forming area. The tangential tensile stress promotes elongation of the sheet along the contour of the formed shape.
2. Radial Stress (σr) – Tensile: The radial stress acts along the direction from the tool contact point toward the periphery of the clamped sheet. It is also tensile, leading to radial stretching and thinning of the sheet material as it is drawn outward from the forming zone.
3. Through-Thickness Stress (σz) – Compressive (top) and Tensile (bottom): This stress acts across the sheet thickness. The upper surface of the sheet (in direct contact with the tool) is subjected to compressive stress due to the downward force applied by the forming tool, while the lower surface (facing away from the tool) experiences tensile stress as it is stretched. The combined effect of these stresses produces bending and thinning in the deformed region.
4. Shear Stress (τ) – Shear: Shear stresses develop at the interface between the tool and the sheet due to frictional contact and tangential tool motion. These stresses influence material flow, heat generation, and surface finish.

The combined effect of these stresses results in bending, stretching, and shear deformation within the localized contact zone. As the tool continuously moves along the programmed path, this deformation zone propagates across the sheet, causing progressive shaping of the material into the desired form without requiring a die.

The process may be conducted at room temperature (cold ISF) or at elevated temperatures (warm/hot ISF), depending on the material's ductility and forming characteristics. Proper lubrication between the tool and sheet minimizes frictional resistance, prevents surface damage, and enhances surface quality.

In summary, the working principle of Incremental Sheet Forming involves the controlled application of tensile, compressive, and shear stresses in a localized region through CNC-

guided tool movement. The superposition of these stresses induces plastic deformation layer by layer, resulting in the gradual formation of the desired three-dimensional geometry.

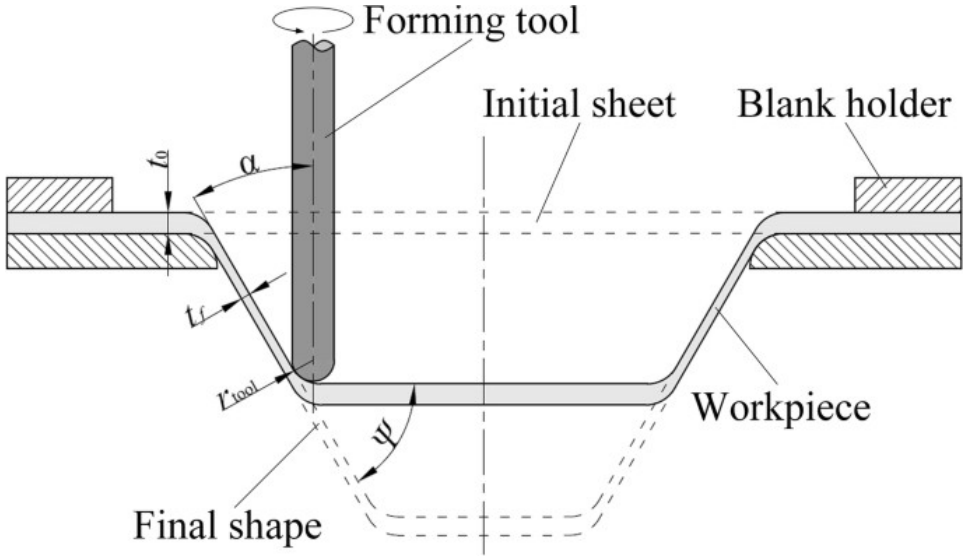

Fig 1: Incremental sheet forming

1.2 History of Development

The development of Incremental Sheet Forming (ISF) has evolved over several decades as an alternative to conventional sheet metal forming methods. The concept originated in the 1960s, when Leszak (1967) first patented a die less forming process that involved shaping sheet metal incrementally using a simple tool. Although innovative, the idea did not gain much industrial use at that time due to the absence of precise computer-controlled machinery.

In the 1980s and early 1990s, the introduction of Computer Numerical Control (CNC) technology made it possible to accurately control the tool movement in multiple directions. This advancement revived interest in incremental forming, allowing researchers to develop processes capable of producing complex geometries without the need for dedicated dies.

By the mid-1990s, significant research by Jeswiet, Matsubara, and other scholars led to the formal development of the two major ISF variants — Single Point Incremental Forming (SPIF) and Two Point Incremental Forming (TPIF)**.** Their work demonstrated the practicality of forming complex shapes through controlled, localized deformation using CNC-based tools.

During the 2000s, ISF became a major research topic in advanced manufacturing. Studies focused on understanding the deformation mechanics, toolpath generation, and formability limits of different materials such as aluminum, steel, and titanium. The process also began to find potential applications in industries like aerospace, automotive, and biomedical engineering.

In the 2010s and beyond, the development of Finite Element Analysis (FEA)**,** robotic forming system**s**, and hybrid techniques such as warm and laser-assisted ISF further improved accuracy, surface quality, and material formability. Recent work integrates ISF with automation, digital control, and AI-based optimization, making it a key technology for customized and flexible manufacturing in the modern industry.

1.3 Applications

i. Cranial Implant Fabrication

- ISF is extensively used in producing patient-specific cranial implants for cranio-maxillofacial reconstruction.
- These implants restore skull defects caused by trauma, tumour removal, or congenital abnormalities.
- ISF enables forming of complex and customized geometries without requiring dedicated dies, making it ideal for medical customization.

ii. Use of Medical Imaging for Implant Design

- CT or MRI scan data of the patient's skull are converted into a 3D CAD model.
- A corresponding toolpath is generated and executed on a CNC machine.
- The forming tool incrementally shapes a biocompatible perforated sheet (e.g., titanium or SS304L) to precisely match the cranial defect.

iii. Advantages of Perforated Sheets in Implants

- Perforations promote bone tissue ingrowth and osseointegration, improving implant stability.
- They allow fluid circulation and ventilation, reducing infection risks.
- Perforated sheets create lightweight implants, lowering mechanical load on the skull.

iv. Benefits of ISF for Forming Perforated Sheets

- ISF provides localized deformation, preventing damage to perforations during forming.
- Structural integrity and biocompatibility of the material are maintained.
- Accurate reproduction of complex cranial geometry is achieved by controlling step size, feed rate, tool diameter, and other parameters.

v. Extension to Other Biomedical Components

- ISF concepts are also used in fabricating maxillofacial plates for facial bone reconstruction.
- It is applied in orthopaedic supports and fixation devices that require customized shaping.
- Perforated surgical meshes and similar biomedical products benefit from the same controlled formability.

vi. Most Prominent Medical Application

- Among various biomedical uses, cranial reconstruction remains the most significant and technically important application of ISF.

Fig 2: Cranial and Facial implants

1.4 Advantages and Disadvantages

Incremental Sheet Forming offers a wide range of advantages that make it an attractive alternative to conventional forming methods:

- Advantages:

- Patient-Specific Customization: Incremental Sheet Forming enables the production of implants that exactly replicate the patient's skull contour using CT or MRI-based digital models. This ensures a precise anatomical fit, better aesthetic restoration, and improved patient comfort after implantation.

- No Need for Dedicated Dies: ISF is a die less process, meaning it does not require expensive, shape-specific dies or molds. This makes it ideal for one-off or low-volume biomedical manufacturing, especially where each implant must be customized to individual patient anatomy.

- Lightweight and Biocompatible Implants: The use of perforated sheets, typically made of titanium or stainless steel (SS304L), results in lightweight implants with high biocompatibility. The perforations promote bone tissue growth through the holes, supporting osseointegration and long-term stability of the implant.

- High Geometrical Flexibility: ISF allows the forming of complex and irregular cranial geometries that are difficult to achieve using conventional forming processes. The CNC-controlled toolpath ensures accurate reproduction of curved skull surfaces and intricate anatomical details.

- Cost-Effective Manufacturing: Since the process requires minimal tooling and setup, it significantly reduces overall production cost. This makes ISF a practical and economical approach for patient-specific cranial implant fabrication compared to traditional manufacturing methods.

1.4.2. Disadvantages:

- Dimensional Inaccuracy and Spring back: Due to localized plastic deformation, the formed implant may exhibit slight geometric deviations or spring back after forming. Minor finishing or adjustment may be necessary to achieve the exact cranial curvature.
- Thickness Reduction: The incremental deformation process causes stretching of the sheet, which can lead to non-uniform thickness distribution. Excessive thinning may affect the mechanical strength and durability of the implant.
- Surface Roughness: Continuous contact between the forming tool and the sheet can leave marks or surface irregularities. Biomedical implants often require additional surface finishing or polishing to meet medical standards.
- Longer Forming Time: Since ISF operates layer by layer with small incremental steps, it is relatively time-consuming compared to conventional stamping or deep drawing. However, the higher forming time is acceptable for customized, one-off medical components.

CHAPTER 2:
LITERATURE REVIEW

2.1 Literature Review

Incremental Sheet Forming (ISF), especially the Single Point Incremental Forming (SPIF) technique, has gained significant attention due to its flexibility, reduced tooling requirements, and ability to form complex geometries. Research in this field has mainly focused on improving formability, understanding deformation behaviour, analysing process parameters, and developing advanced numerical models.

One of the earlier studies on stainless steels was conducted by A. Chennakesava Reddy (2017) in the paper "Experimental and Numerical Studies on Formability of Stainless Steel 304 in Incremental Sheet Metal Forming of Elliptical Cups." This work demonstrated that wall angle, step size, and tool diameter significantly influence thinning and fracture in SS304 during ISF. Similarly, the study "Revisiting Formability and Failure of AISI 304 Sheets in SPIF: Experimental Approach and Numerical Validation" by Gabriel Centeno et al. (2017) examined the failure mechanisms of AISI 304 and successfully validated numerical predictions with experiments.

The influence of parameters on forming forces was explored by Ajay Kumar et al. (2020) in their work "Parametric Investigation of Forming Forces in Single Point Incremental Forming." They reported that tool radius, step depth, spindle speed, and feed rate directly impact forming forces. Manish Oraon et al. (2020) in "Investigation into the Process Parameter of Single Point Incremental Forming (SPIF)" also emphasized that step depth and tool size greatly affect accuracy and deformation quality. A deeper analytical understanding of contact mechanics was later presented by Hui Zhu and Hengan Ou (2025) in "Analytical Modelling of Local Contact behaviour in Incremental Sheet Forming," where a predictive model for tool-sheet contact forces was developed.

Many recent works have focused on perforated sheet metals due to their high flexibility. Anees Jaleel and C. Sathiya Narayanan (2023) investigated perforated SS304L in the paper "Formability Investigation of Perforated Austenitic SS304L Sheets Using SPIF." They concluded that perforation size and pitch significantly modify strain paths. Their second paper, "Optimization, Finite Element Simulation, Fractography and Tool Wear Analysis During SPIF Process of Perforated Stainless-Steel Sheets" (2023), further explored FE modeling,

fractography, and optimized processing conditions. Other contributions include “Research on Single Point Incremental Forming Characteristics of Perforated TA1 Sheet” by Ruxiong Li & Tao Wang (2022) and “Formability Improvement in Die-Less Forming Process of Ti Gr. 2 Perforated Sheet: Experiment Method and Finite Element Analysis” by Rahul R. Gurpude et al. (2025), both highlighting improved ductility and reduced forming force requirements in perforated titanium materials. Perforated sheets have also been explored for biomedical use, as shown in “Patient-Specific Cranial Implant Fabrication: Evaluating Single-Point Incremental Forming with Perforated Titanium Grade-2 Sheets” by Saurabh Thakur and Sant Ram Chauhan (2015).

Titanium and its alloys remain important in SPIF research due to their application in aerospace and biomedical implants. Valentin Oleksik et al. (2021) provided a broad study titled “Single-Point Incremental Forming of Titanium and Titanium Alloy Sheets,” summarizing challenges such as low room-temperature ductility. C. Veera Ajay (2020) optimized SPIF parameters for titanium alloys in the paper “Parameter Optimization in Incremental Forming of Titanium Alloy Material.” The role of forming speed was evaluated by E. H. Uheida et al. (2017) in “Investigating the Impact of Velocity on the Process Conditions in Incremental Forming of Titanium Sheets,” revealing that higher speeds improve formability through localized heating. Additionally, Antonio Piccininni et al. (2016) combined superplastic forming and ISF in their work “Biomedical Titanium Alloy Prostheses Manufacturing by Means of Superplastic and Incremental Forming Process,” demonstrating improved accuracy in biomedical components.

Advanced material behaviour during SPIF was analysed by Elizabeth M. Mamros et al. (2024) in the paper “Martensitic Transformation of SS304 Truncated Square Pyramid Manufactured by Single Point Incremental Forming.” This study confirmed that strain-induced martensite improves formability and strength. Their related work, “Investigation Using Single Point Incremental Forming (SPIF) to Fabricate Patient-Specific Titanium Orbital Floor Implants,” showcased the capability of SPIF in producing customized medical implants.

Comparison between conventional forming and SPIF was done by Seyyed Emad Seyyedi et al. (2023) in their study “Comparison Between Conventional Press-Working and Incremental Forming in Hole Flanging of AA6061-T6 Sheets Using a Ductile Fracture Model.” They concluded that SPIF offers higher formability but requires accurate fracture prediction to avoid failure.

Overall, the literature indicates that SPIF is a flexible and highly adaptable process with applications in aerospace, automotive, and biomedical engineering. Key factors influencing formability include tool size, step depth, feed rate, sheet thickness, and perforation patterns. Numerical modelling, fractographical studies, and material transformation analyses continue to enhance process understanding and optimization.

2.2 Literature Gap

Although many studies have investigated Single Point Incremental Forming (SPIF), the existing literature shows several gaps, especially for perforated SS304L sheets. Previous works such as those by Anees Jaleel & Sathiya Narayanan (2023) and Ruxiong Li & Tao Wang (2022) mainly focus on experimental formability of perforated sheets, but they provide limited numerical analysis using finite element simulation. Most researchers have studied either forming forces, strain behaviour, or thickness variation separately, but not all these factors together for perforated stainless steels.

Studies on stainless steel SPIF, such as those by Chennakesava Reddy (2017) and Gabriel Centeno et al. (2017), concentrate on non-perforated SS304 sheets. These do not capture the unique deformation behaviour caused by perforations, such as localized strain concentration, reduced stiffness, and different thinning patterns. Similarly, works like Ajay Kumar et al. (2020) analyse forming forces, but mainly for solid sheets and without considering the combined effect of feed rate, step depth, and spindle speed on perforated materials. Numerical modelling guidelines, tool–sheet contact behaviour, and stress distribution for perforated stainless steel are also not sufficiently reported.

Overall, there is very limited numerical simulation research that studies how multiple SPIF process parameters affect contact forces, strain distribution, sheet-thickness variation, and von-Mises stress specifically in perforated SS304L sheets. There is also a lack of simulation studies that are planned specifically to be verified later through experiments using the same perforation pattern and forming conditions.

The present work addresses these gaps by performing a detailed finite element simulation of incremental forming of perforated SS304L sheets using Abaqus, considering variations in feed rate, step depth, and spindle speed. The study compares key outputs such as contact forces, strain diagrams, thickness reduction, and von-Mises stress, which are not comprehensively

available in previous literature for perforated SS304L. This simulation work also sets a foundation for future experimental validation, making the results more reliable and practically useful.

2.3 Objective Formulation

The present work focuses on understanding the formability of perforated SS304L sheets under the Single Point Incremental Forming (SPIF) process. The study involves both numerical simulation using Abaqus/CAE and experimental validation using a CNC machine. Different process parameters such as feed rate, step depth, and spindle speed are varied to observe their effect on sheet deformation and forming behaviour.

The specific objectives of the study are outlined below:

- Examine the formability and deformation behaviour of perforated SS304L sheets during the SPIF process.
- Analyse how variations in feed rate, step depth, and spindle speed influence forming depth, strain distribution, and surface quality.
- Conduct finite element simulations in Abaqus/CAE to study stress, strain, and thickness variation under different process settings.
- Validate the simulation results through experimental trials on a CNC machine and compare both outcomes for accuracy and correlation.

2.4 Methodology / Work Plan

This work focuses on studying the formability of perforated SS304L sheets under the Single Point Incremental Forming (SPIF) process through both numerical simulation and experimental validation. The simulation stage was performed in Abaqus/CAE, and the experimental stage will be conducted using a CNC milling machine to verify the results.

- A finite element model of the SPIF setup was created in Abaqus/CAE, with the sheet modelled as a deformable shell and the forming tool as an analytical rigid body.

- The spiral toolpath required for forming was designed in Autodesk Fusion 360 and imported into Abaqus for simulation.
- The material behaviour of SS304L was defined using Hollomon's law ($\sigma = K\varepsilon^n$) to represent elastic–plastic deformation with strain hardening.
- Simulations were carried out by varying feed rate, step depth, and spindle speed, while other parameters were kept constant.
- The results were analysed for stress, strain, thickness variation, and forming depth, and will be validated experimentally to compare deformation behaviour and accuracy.
- Properties of SS304L are taken as :

Table 1 : Mechanical properties of SS304L

Sl.No.	Properties	2mm φ hole sheet
1	Strength coefficient, K	647.294 MPa
2	Strain hardening exponent, n	0.349
3	Ultimate tensile strength	374 MPa
4	Yield strength	277 MPa
5	Elasticity	195000 MPa

CHAPTER 3:

EXPERIMENTAL DETAILS / MODEL DEVELOPMENT

3.1 Experimental Studies

The present work focuses on the simulation and validation of incremental sheet forming (ISF) of perforated SS304L sheets. The experimental studies are carried out using a CNC milling machine, which is used to replicate the forming process observed in the numerical simulation. The aim of the experiments is to validate the simulation results obtained from Abaqus CAE and to analyse the influence of different process parameters on the formability of the perforated sheet.

3.1.1 Materials

The workpiece material used for the study is SS304L stainless steel, selected for its excellent formability and corrosion resistance, making it suitable for biomedical applications. The sheet used has perforations arranged in a regular pattern to study their effect on deformation behavior during forming.

The material behaviour of SS304L is defined using Hollomon's law, expressed as:

$$\sigma = K\varepsilon^n$$

where,

σ= true stress,

ε= true strain,

K= strength coefficient,

n= strain hardening exponent.

The mechanical properties of SS304L, including Young's modulus, Poisson's ratio, and density, are defined based on standard literature values.

3.2 Model development

The development of the experimental setup for incremental sheet forming (ISF) involves preparing all necessary equipment, fixtures, and toolpath information to accurately reproduce the forming process. A 3-axis CNC milling machine will be used as the primary forming platform, with the forming tool mounted on the machine spindle. A custom-designed clamping fixture will be fabricated to securely hold the perforated SS304L sheet and prevent any

movement during forming. The toolpath required for shaping the sheet will be generated in Autodesk Fusion 360 based on the desired geometry, and the corresponding G-code will be transferred to the CNC controller. Proper alignment of the sheet, calibration of tool position, and verification of spindle rotational speed settings will be carried out before forming begins. This setup ensures stable sheet support, accurate tool movement, and reliable replication of the planned incremental forming process.

3.2.1 CAD Model Development

The forming geometry considered in this study is a truncated cone. A surface model of the geometry was created in SolidWorks to replicate the forming profile rather than a full solid volume. Surface modelling was chosen because it allows easier definition of toolpath trajectories for incremental forming processes and ensures compatibility with downstream toolpath generation. The surface geometry was then exported in a format suitable for use in Fusion for toolpath creation.

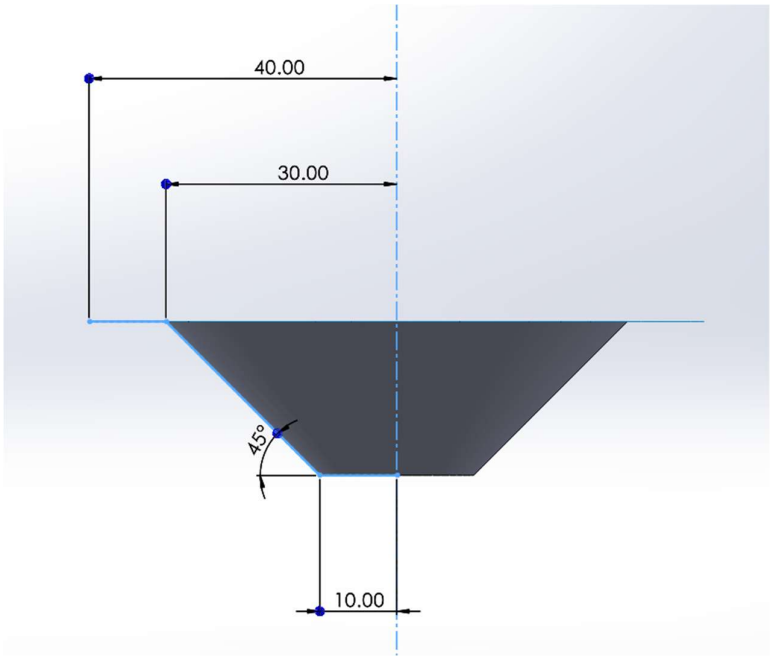

Fig 3: CAD model designed in SolidWorks (with dimensions)

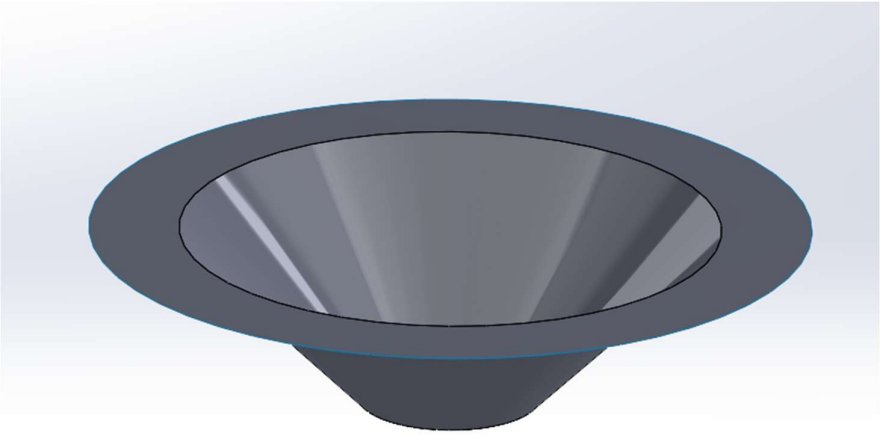

Fig 4: CAD model designed in SolidWorks (isometric view)

3.2.2 Forming Tool

A hemispherical forming tool made of hardened steel is used for the experiments. The tool parameters such as diameter and surface finish are kept constant for all trials to ensure consistency in results.

3.2.3 Process Parameters

The forming process is carried out by varying the following key process parameters:

- Feed rate (mm/min)
- Spindle speed (rpm)
- Step depth (mm)

These parameters are systematically changed to study their effect on the sheet's deformation behaviour, surface quality, and overall formability.

3.2.4 Toolpath Generation

The toolpath for the incremental forming process was generated using Autodesk Fusion 360. A spiral toolpath strategy was selected to ensure continuous and uniform deformation. The following parameters were used for toolpath definition:

- Step size: 0.2 mm

- Forming tool type: Ball end tool (hemispherical tip)
- Tool diameter: 10 mm
- Feed rate: 800 mm/min
- Spindle speed: 300 rpm

As shown in the fig. 2, the toolpath consisted of successive spiral passes corresponding to incremental depth and wall angle increases. The generated toolpath coordinates were exported and later imported into Abaqus CAE to define the tool movement during simulation.

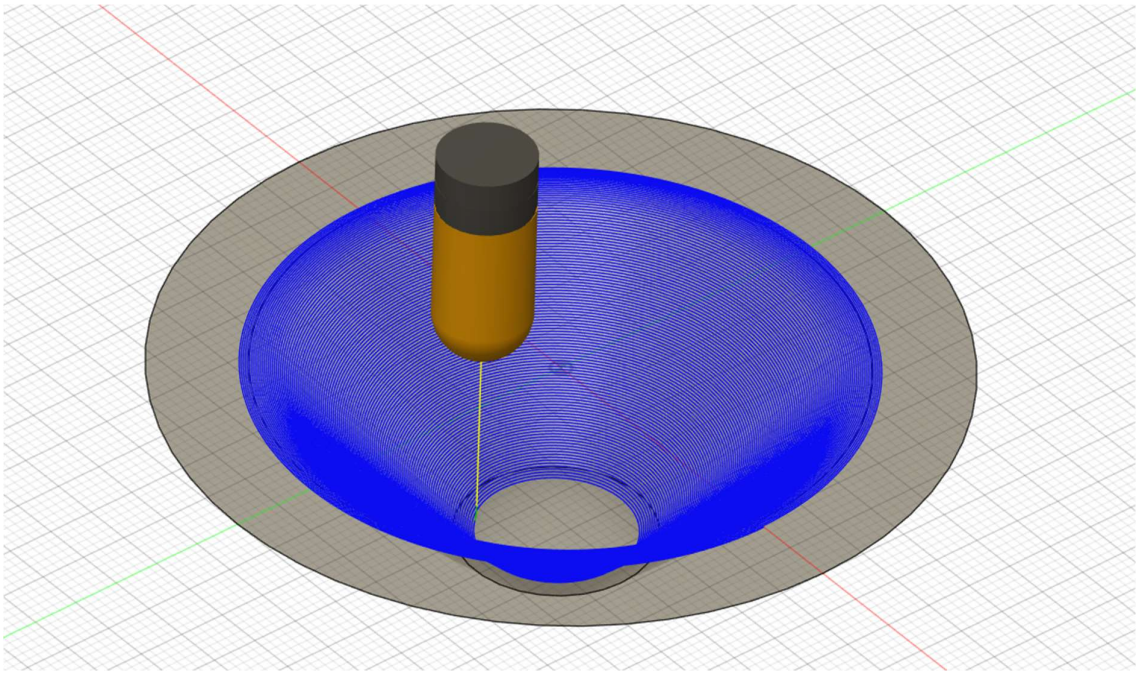

Fig. 5: Toolpath taken from Autodesk Fusion

3.2.5 Simulation Platform

The simulations were carried out using Abaqus/CAE (Dassault Systèmes, Version 2020). The forming tool was modelled as an analytical rigid ball end tool with a hemispherical profile. The perforated SS sheet was modelled as a deformable shell with material properties corresponding to SS 304L, including elastic modulus, Poisson's ratio, yield strength, and plastic strain data available from standard references.

3.2.6 Boundary Conditions

In the simulation, six boundary conditions were applied to accurately represent the incremental sheet forming setup. An ENCASTRE boundary condition was assigned to fully fix the fixture

and prevent any unwanted movement. The forming tool motion was defined using the toolpath imported from Fusion 360, where the X, Y, and Z displacements were applied through amplitude curves representing position versus time. To ensure realistic tool behaviour, rotational motion of the tool was restricted about the X and Y axes, while a rotational velocity corresponding to the required spindle speed (rpm) was applied about the Z-axis. These boundary conditions collectively ensured proper replication of the actual CNC forming process within the simulation environment.

3.2.6 Meshing and Analysis

The perforated SS304L sheet was meshed using S4R shell elements to capture large deformation behaviour accurately. A global seed size of 10 mm was applied along with curvature and minimum-size control to maintain mesh quality around perforations. The analysis was performed in Abaqus using nonlinear geometry, toolpath-based loading, and appropriate contact definitions to simulate the incremental forming process realistically.

- S4R shell elements were used with a global seed size of 10 mm to create a uniform mesh. Curvature refinement was applied to generate smaller elements around hole edges and curved regions.
- Minimum size control was included to prevent overly large or distorted elements in critical areas. This ensured better accuracy around perforations and improved overall mesh quality.
- Mesh smoothness was ensured by avoiding abrupt transitions between coarse and fine areas. This improved solver stability and reduced the risk of convergence issues.

CHAPTER 4:
RESULTS AND DISCUSSION

4.1 Contact force magnitude (CFNM)

4.1.1 Upon changing feed rates

The CFNM plots for feed rates of 600, 800, and 1000 mm/min show a progressive increase in peak contact force as the forming speed increases. At 600 mm/min, the maximum contact force reaches 1036.331 N at approximately 1266.426 s, with relatively smoother fluctuations throughout the process. For 800 mm/min, the peak force increases to 1155.196 N, occurring earlier at around 877.105 s, indicating a stronger and more rapid interaction between the tool and sheet. At the highest feed rate of 1000 mm/min, the contact force reaches its maximum value of 1237.106 N at about 794.668 s, accompanied by more intense and frequent fluctuations. This overall trend demonstrates that higher feed rates lead to larger peak forces and greater force variability due to faster deformation and reduced material response time during incremental sheet forming.

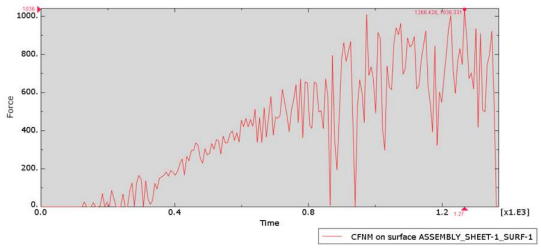

Fig 6: Contact Force v/s time plot (600 mm/min)

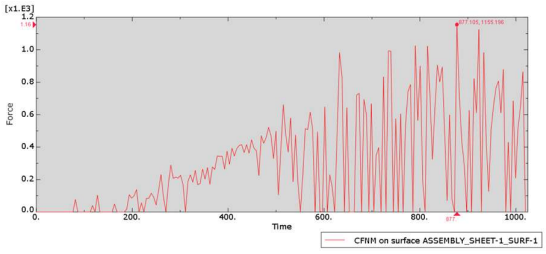

Fig 7: Contact Force v/s time plot (800 mm/min)

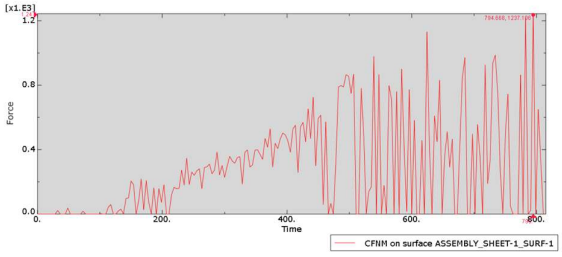

Fig 8: Contact Force v/s time plot (1000 mm/min)

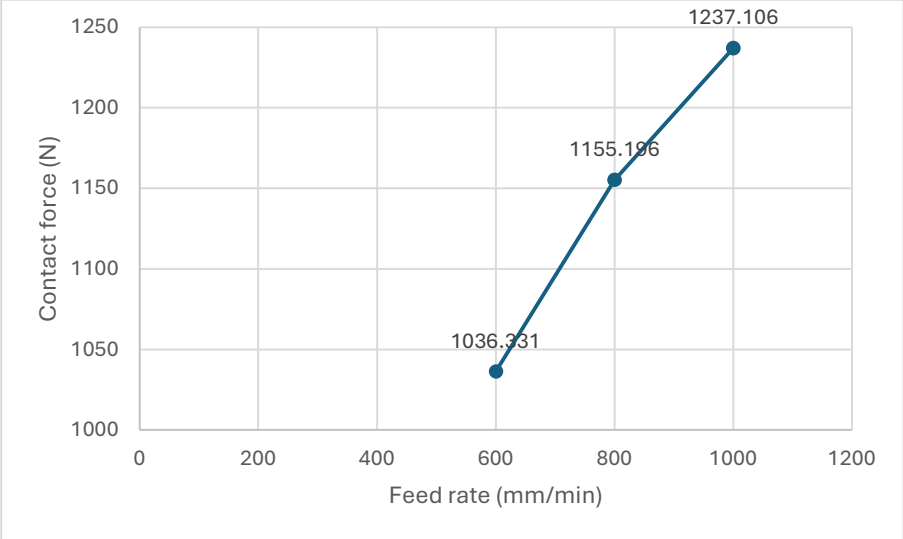

Fig 9: Contact Force v/s feed rate plot

4.1.2 Upon changing step depth

The CFNM plots for step depths of 0.1 mm, 0.2 mm, and 0.3 mm show a clear difference in force levels and the time at which peak forces occur. At 0.1 mm, the contact force reaches the highest value among the three conditions, with a peak of 1825.294 N at around 1132.654 s, indicating that even though deformation per step is low, the tool maintains longer contact, resulting in a higher cumulative peak force. For 0.2 mm, the maximum force recorded is 1155.196 N at approximately 877.105 s, showing a moderate force level and earlier peak compared to the 0.1 mm case. At 0.3 mm, the maximum contact force is 1183.371 N, occurring even earlier at roughly 666.925 s, which reflects faster material penetration and increased resistance due to larger incremental deformation per step. Overall, the comparison shows that smaller step depths lead to higher peak forces over a longer forming time, while larger step depths produce peak forces more quickly but with slightly lower force values relative to the 0.1 mm condition.

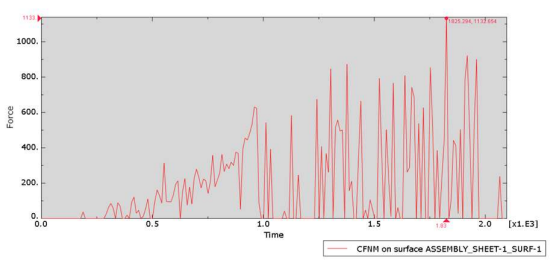

Fig 10: Contact Force v/s time plot (0.1 mm)

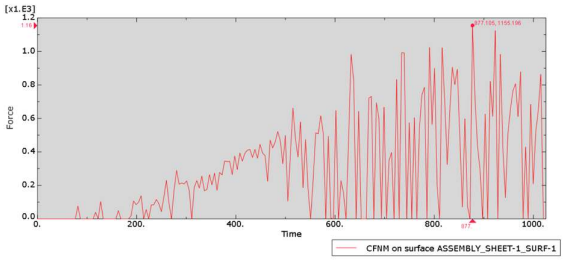

Fig 11: Contact Force v/s time plot (0.2 mm)

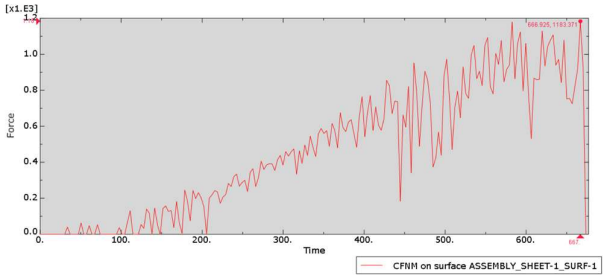

Fig 12: Contact Force v/s time plot (0.3 mm)

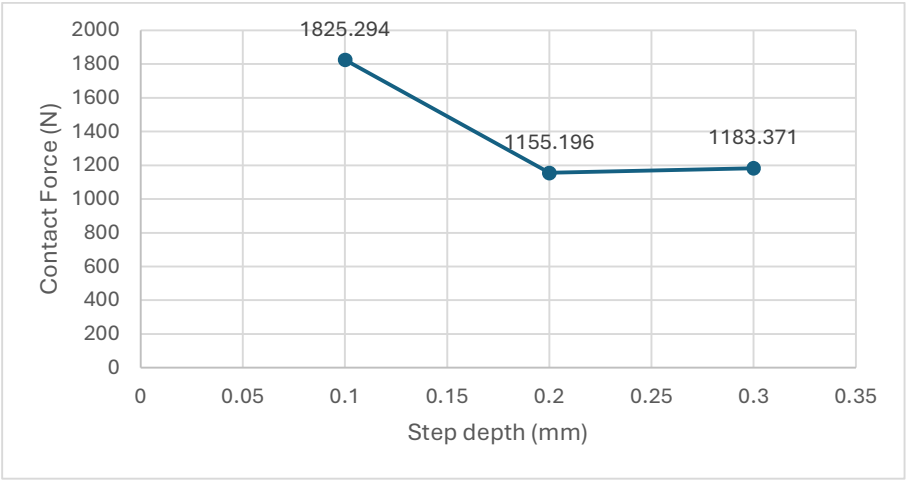

Fig 13: Contact Force v/s step depth plot

4.1.3 Upon changing speed of tool (rpm)

The CFNM plots for spindle speeds of 200, 300, and 400 rpm show noticeable differences in the magnitude and timing of peak forming forces during the incremental sheet forming process. At 200 rpm, the maximum contact force reaches 1187.15 N at around 877.105 seconds, indicating relatively high resistance due to slower rotation, which allows deeper tool–sheet interaction. For 300 rpm, the peak force decreases slightly to 1155.196 N, also occurring at approximately 877.105 seconds, showing that a moderate spindle speed reduces the required forming force while maintaining a similar forming duration. At 400 rpm, the maximum force increases again to 1283.657 N, occurring earlier at around 815.912 seconds, suggesting that higher rotation speeds intensify the tool–sheet contact, resulting in faster force development and greater local resistance. Overall, the comparison shows that 300 rpm provides the lowest

peak force, while 400 rpm produces the fastest and highest force rise, demonstrating that spindle speed strongly influences forming load and deformation behaviour.

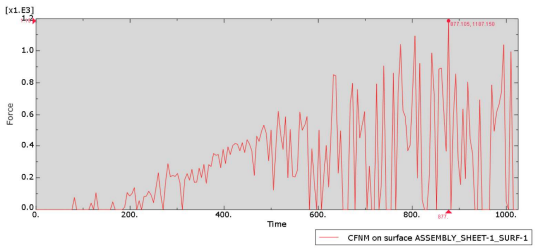

Fig 14: Contact Force v/s time plot (200 rpm)

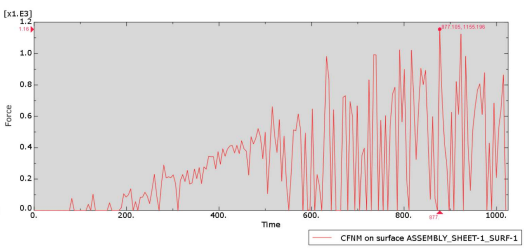

Fig 15: Contact Force v/s time plot (300 rpm)

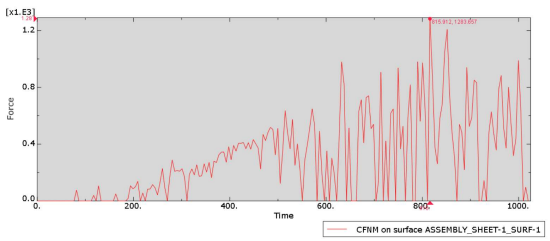

Fig 16: Contact Force v/s time plot (400 rpm)

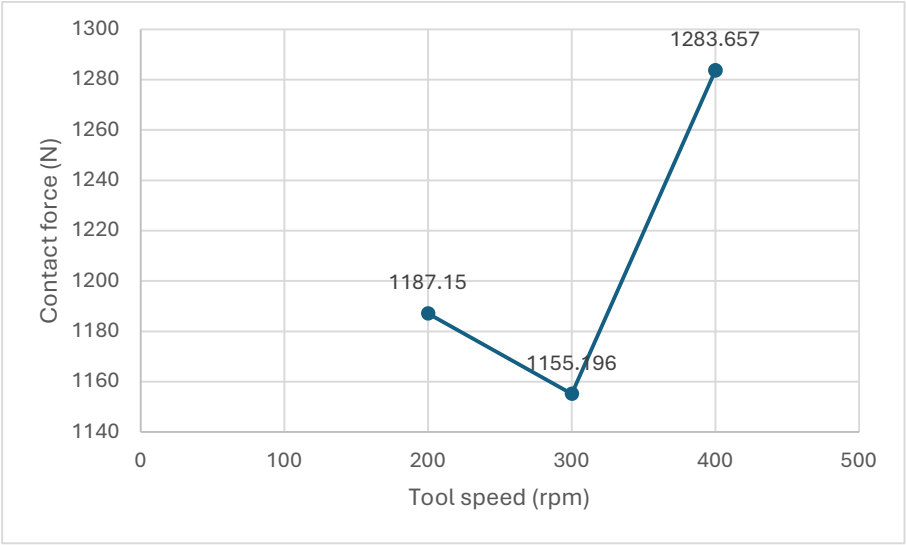

Fig 17: Contact Force v/s tool speed in rpm plot

4.2 Sheet Thickness

4.2.1 Upon changing feed rates

The sheet-thickness plots for 600, 800 and 1000 mm/min clearly show that increasing the feed rate accelerates thinning of the material. At 600 mm/min, thickness remains almost constant at

≈1.00 mm for most of the forming time and begins to drop only after around 0.9 × 10^3 s, finally reaching ≈0.76 mm. At 800 mm/min, thinning starts earlier, around 0.6 × 10^3 s, and the sheet thickness gradually decreases until it reaches ≈0.60 mm by 1000 s, showing a much sharper decline compared to 600 mm/min. For the highest feed rate of 1000 mm/min, thickness deterioration is even more rapid: although the sheet stays close to 1.00 mm initially, thinning starts near 0.55–0.60 × 10^3 s and quickly drops to ≈0.75 mm by 0.8 × 10^3 s. Overall, higher feed rates result in earlier onset of thinning and a lower final sheet thickness, indicating that rapid tool motion increases material stretching and reduces the sheet's ability to maintain uniform thickness.

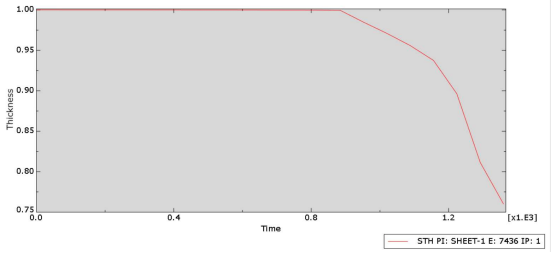

Fig 18: Sheet thickness v/s time plot (600 mm/min)

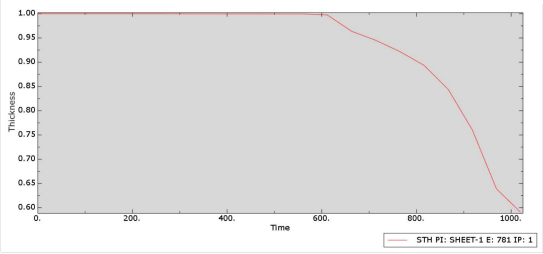

Fig 19: Sheet thickness v/s time plot (800 mm/min)

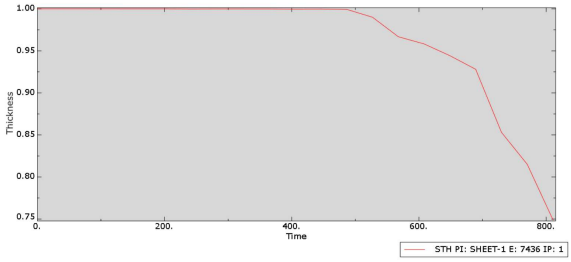

Fig 20: Contact Force v/s time plot (1000 mm/min)

Table 2: Thickness drop characteristic upon varying feed rate

Feed rate (mm/min)	**Sheet thickness (mm)**	**Time of completion**	**Thickness change duration**	**Thickness drop characteristic**
600	0.75	1359.853	600 – 1359	Gradual
800	0.6	1019.889	600 – 1019	Sharp
1000	0.75	810.885	500 – 810	Very sharp

4.2.2 Upon changing step depth

The thickness-versus-time plots for 0.1, 0.2, and 0.3 mm step depths show that greater step depth leads to faster and more severe thinning of the sheet. At a 0.1 mm step depth, the sheet retains close to its original thickness (≈1.0 mm) for most of the forming time and only begins to thin after around 2000 seconds, dropping to about 0.71 mm near the end. At a 0.2 mm step depth, thinning starts much earlier (around 600 seconds) and progresses more aggressively, reducing the thickness from 1.0 mm to nearly 0.60 mm by 1000 seconds, indicating much higher deformation. At the largest step depth of 0.3 mm, the sheet rapidly loses thickness after 400 seconds, reaching just ≈0.58 mm by ~650 seconds, which is the fastest and most drastic reduction among the three. Overall, increasing the step depth significantly accelerates thinning and reduces the minimum achievable thickness, clearly showing that deeper incremental forming steps impose higher deformation and material loss.

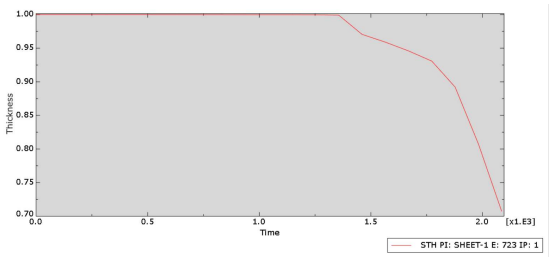

Fig 21: Sheet thickness v/s time plot (0.1 mm)

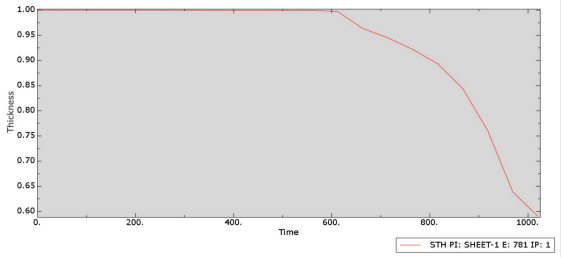

Fig 22: Sheet thickness v/s time plot (0.2 mm)

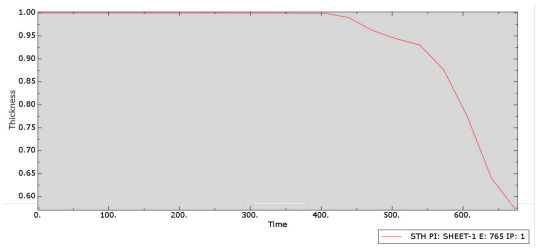

Fig 23: Sheet thickness v/s time plot (1000 mm/min)

Table 3: Thickness drop characteristic upon varying step depth

Step depth (mm)	Sheet thickness (mm)	Time of completion	Thickness change duration	Thickness drop characteristic
0.1	0.7	2046.047	1200 - 2046	Gradual
0.2	0.6	1019.889	600 – 1019	Sharp
0.3	0.625	673.662	400 – 673	Very sharp

4.2.3 Upon changing speed of tool (rpm)

The sheet-thickness variation trends indicate that increasing spindle speed accelerates thinning of the perforated SS304L sheet during incremental sheet forming. At 200 rpm, the sheet retains nearly its original thickness (~1.00 mm) for most of the forming duration and a noticeable drop begins only after around 700–750 s, finally reaching a minimum thickness of approximately 0.65 mm near 1000 s. At 300 rpm, the thinning begins earlier and proceeds more aggressively; although the sheet again starts near 1.00 mm, the thickness reduces steadily after around 650–680 s, dropping to around 0.60 mm by 1000 s. At 400 rpm, the sheet exhibits the most rapid reduction in thickness. Despite starting near 1.00 mm, thinning initiates soon after 600 s, decreasing to around 0.75 mm by 900 s and approaching 0.58 mm by 1000 s. Overall, the analysis shows that higher rpm increases deformation severity and sheet thinning because of greater heat generation, strain rate, and material flow, with 400 rpm leading to the maximum thinning, followed by 300 rpm, while 200 rpm maintains the highest thickness throughout the process.

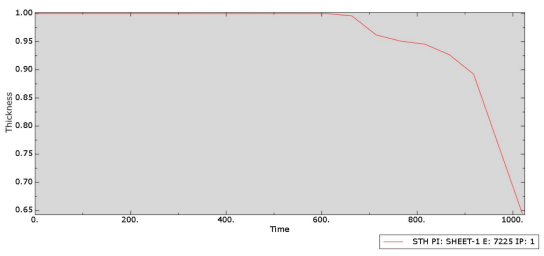

Fig 24: Sheet thickness v/s time plot (200 rpm)

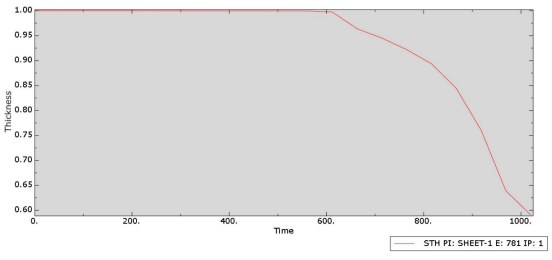

Fig 25: Sheet thickness v/s time plot (300 rpm)

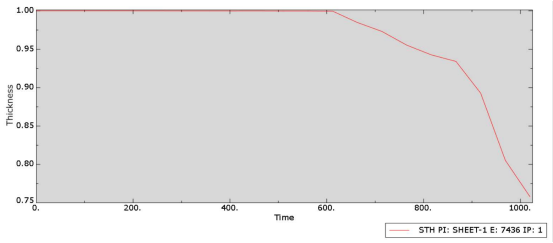

Fig 26: Sheet thickness v/s time plot (400 rpm)

Table 4: Thickness drop characteristic upon varying tool speed

Step depth (mm)	Sheet thickness (mm)	Formability
200	0.65	less
300	0.6	lesser
400	0.75	high

4.3 Von mises stresses

4.3.1 Upon changing feed rates

The von Mises stress contour plots for feed rates of 600, 800, and 1000 mm/min show that the stress response of the sheet does not increase uniformly with feed rate, but instead varies depending on how the material adapts to the forming speed. At 600 mm/min, the maximum von Mises stress reaches approximately 577.8 MPa, indicating significant but stable plastic deformation around the tool path. When the feed increases to 800 mm/min, the maximum stress slightly decreases to about 560.6 MPa, showing that at this intermediate speed, the loading rate allows the material to deform more uniformly with less peak stress concentration. However, at 1000 mm/min, the maximum stress rises again to about 578.9 MPa, nearly matching the 600 mm/min case. This suggests that the higher feed rate causes more aggressive deformation, increasing localized stress and bringing the material closer to its forming limits. Overall, the results show that 800 mm/min produces the lowest peak stress, indicating smoother deformation, while 600 and 1000 mm/min generate higher stress levels, making them comparatively more critical in terms of potential failure risk.

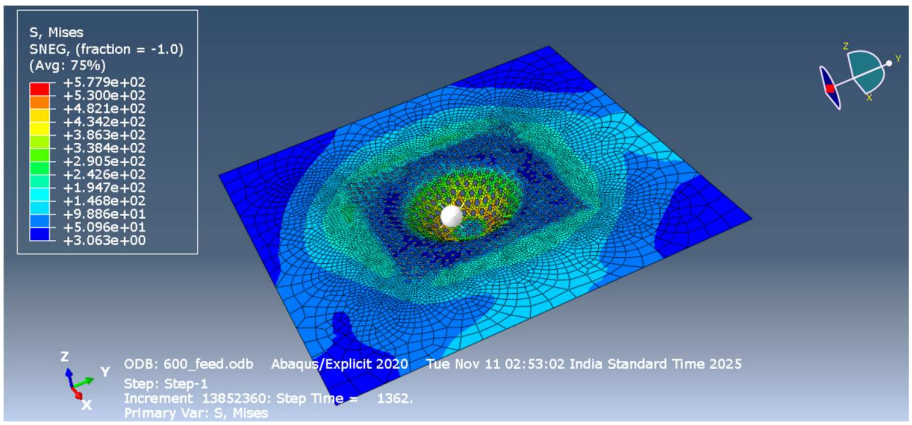

Fig 27: Contour plot of Von mises stress (600 mm/min)

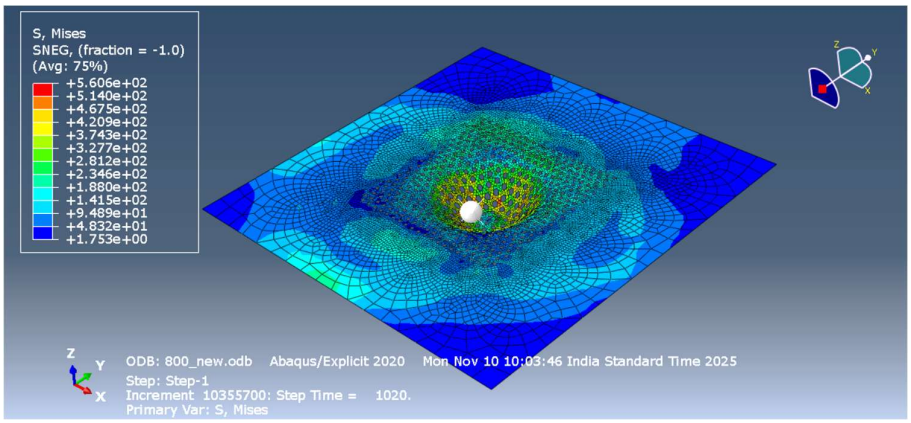

Fig 28: Contour plot of Von mises stress (800 mm/min)

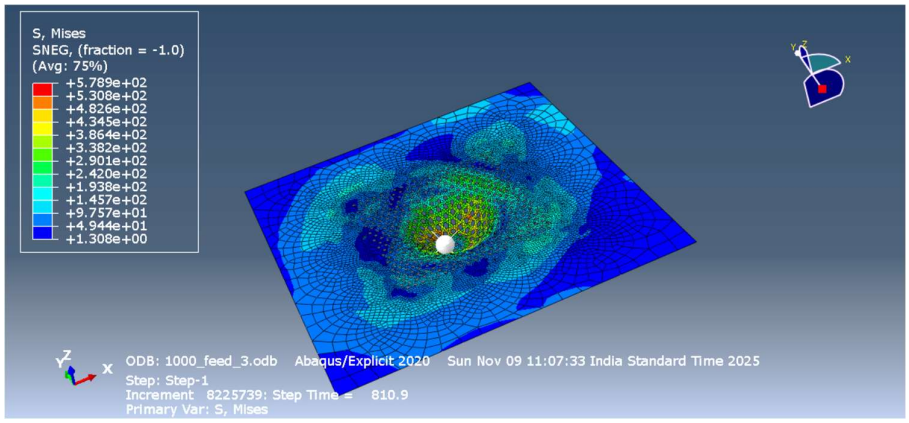

Fig 29: Contour plot of Von mises stress (1000 mm/min)

Table 5: Von mises stress for different feed rates

Feed rate (mm/min)	Max Von Mises stress (MPa)
600	577.8
800	560.6
1000	578.9

4.3.2 Upon changing step depths

The von Mises stress contours for the three step depths (0.1, 0.2, and 0.3 mm) show how the deformation severity changes with incremental tool penetration. At a 0.1 mm step depth, the sheet experiences the highest maximum stress of 580.5 MPa, indicating that the smaller step depth causes more localized plastic deformation because the tool interacts with the sheet for a longer duration. At 0.2 mm, the maximum stress decreases to 560.6 MPa, suggesting a more balanced deformation where the load is distributed more efficiently, resulting in comparatively lower stress concentration. For the 0.3 mm step depth, the maximum stress slightly increases to 568.3 MPa, showing that larger steps introduce sharper deformation but still do not exceed the stress levels at 0.1 mm. Overall, 0.2 mm step depth produces the lowest stress, implying a more stable and efficient forming condition, while 0.1 mm induces the highest stress concentration, and 0.3 mm shows moderate but increasing stress levels due to larger incremental deformation.

Table 6: Von mises stress for different step depths

Step depth (mm)	Max Von Mises stress (MPa)
0.1	580.5
0.2	560.6
0.3	568.3

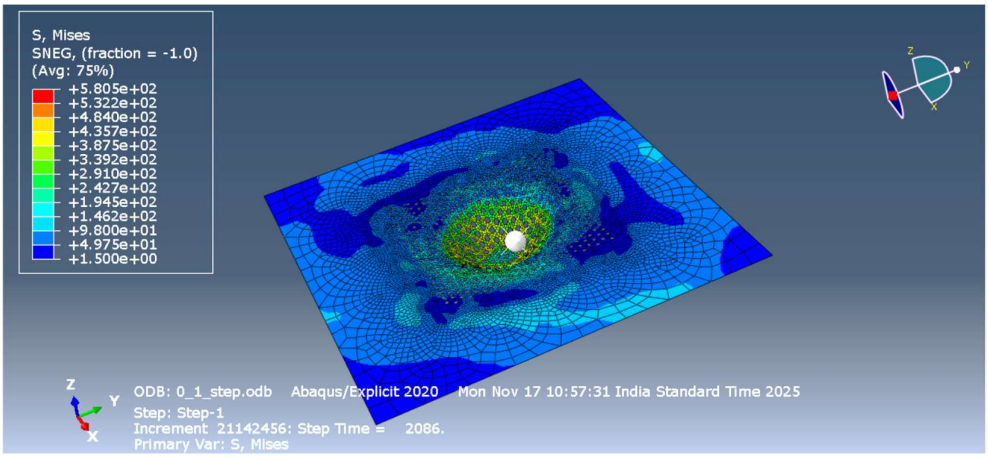

Fig 30: Contour plot of Von mises stress (0.1 mm)

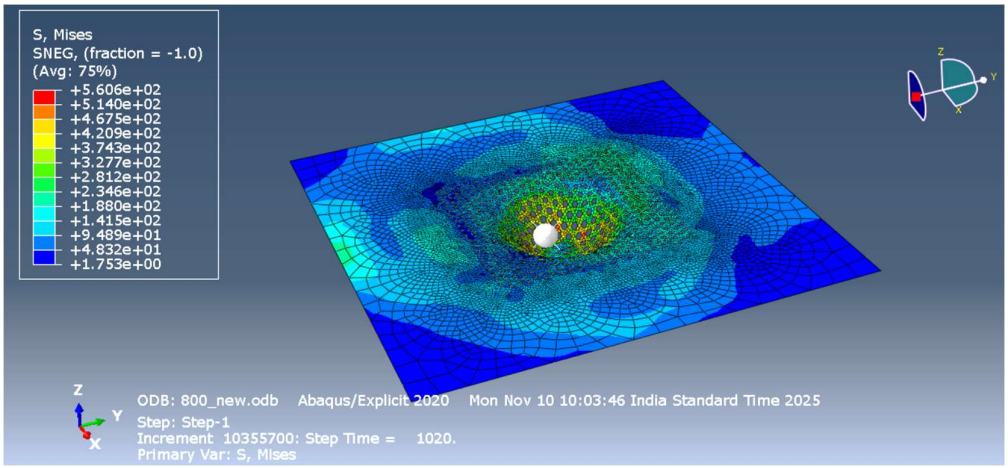

Fig 31: Contour plot of Von mises stress (0.2 mm)

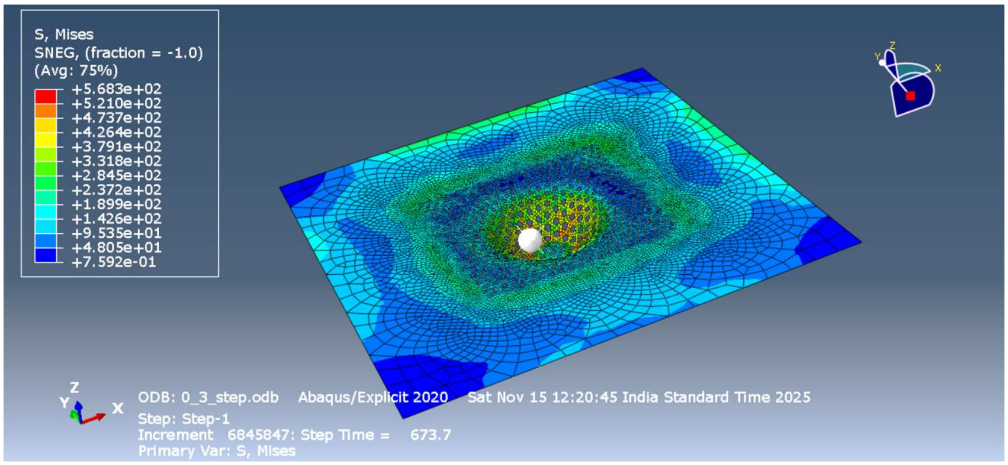

Fig 32: Contour plot of Von mises stress (0.3 mm)

4.3.3 Upon changing Tool speed (rpm)

The von Mises stress distribution for the three spindle speeds shows a noticeable variation in the peak stress levels experienced by the perforated SS304L sheet. At 200 rpm, the sheet records the highest maximum stress of 630.8 MPa, indicating that the deformation process at this lower rotational speed induces greater resistance and higher localized stresses around the tool path. At 300 rpm, the maximum stress reduces significantly to 560.6 MPa, suggesting smoother material flow and a more stable forming condition, making it the least severe loading case among the three speeds. At 400 rpm, the maximum von Mises stress increases slightly to 576.3 MPa, which is higher than 300 rpm but still lower than 200 rpm. This trend shows that very low speed (200 rpm) results in higher stress due to increased contact duration and material resistance, while moderate speed (300 rpm) provides the most balanced and efficient deformation, and higher speed (400 rpm) again increases stress due to faster tool–sheet

interaction and reduced time for material relaxation. Overall, 300 rpm emerges as the most favorable condition, producing the lowest stress and indicating better formability.

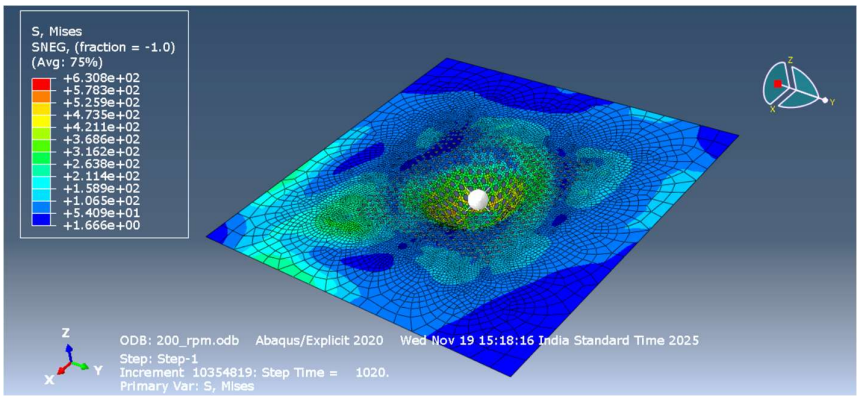

Fig 33: Contour plot of Von mises stress (200 rpm)

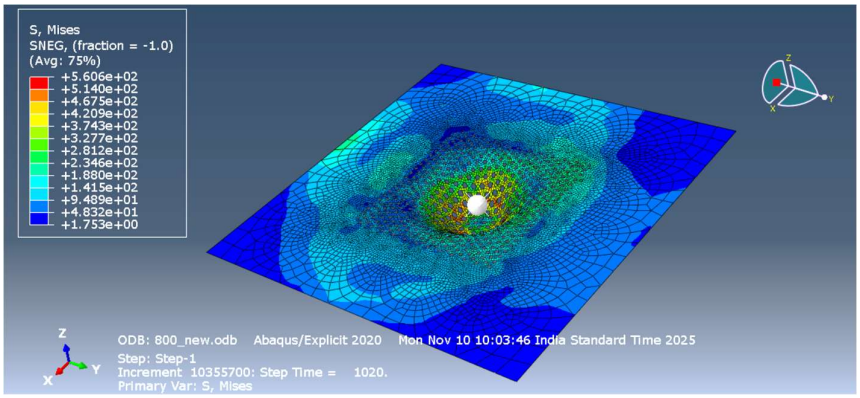

Fig 34: Contour plot of Von mises stress (300 rpm)

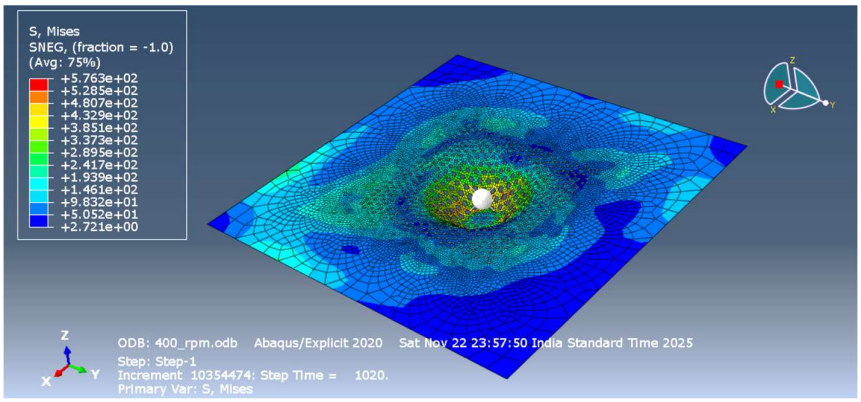

Fig 35: Contour plot of Von mises stress (400 rpm)

Table 7: Von mises stress for different tool speeds

Tool speed (rpm)	Max Von Mises stress (MPa)
200	630.8
300	560.6
400	576.3

4.4 Strain diagram

4.4.1 Upon changing feed rates

The LE11 vs LE22 strain plots for feed rates of 600, 800, and 1000 mm/min show a consistent pattern in which tensile strain (LE11) increases while compressive strain (LE22) becomes more negative as deformation progresses. For the 600 mm/min feed rate, LE11 gradually increases up to approximately 0.40, while LE22 decreases to around –0.10, indicating steady and uniform stretching. At 800 mm/min, LE11 similarly reaches values close to 0.35, with LE22 dropping to nearly –0.15, but the slope of the curve shows slightly sharper strain development compared to 600 mm/min. For the 1000 mm/min condition, LE11 again rises toward 0.38, and LE22 decreases to around –0.13, with a smoother and more linear relationship between the two strains. Overall, the comparison shows that while the strain range across all feed rates remains similar—with LE11 between 0.00–0.40 and LE22 between 0.00 to –0.10—the rate and sharpness of strain development increase with feed rate, indicating that higher feeds promote faster in-plane stretching during incremental sheet forming.

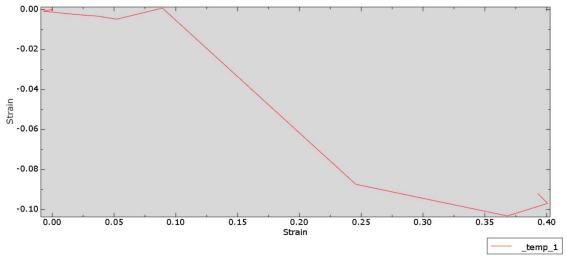

Fig 36: LE11 v/s LE22 plot (600 mm/min)

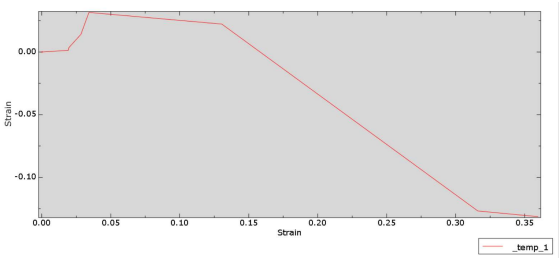

Fig 37: LE11 v/s LE22 plot (800 mm/min)

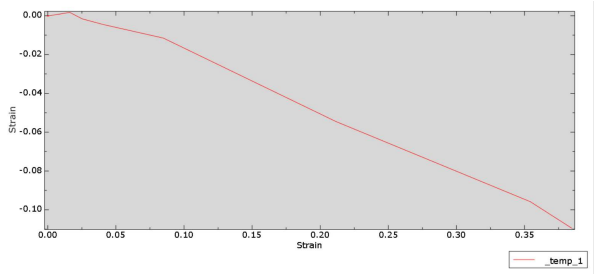

Fig 38: LE11 v/s LE22 plot (1000 mm/min)

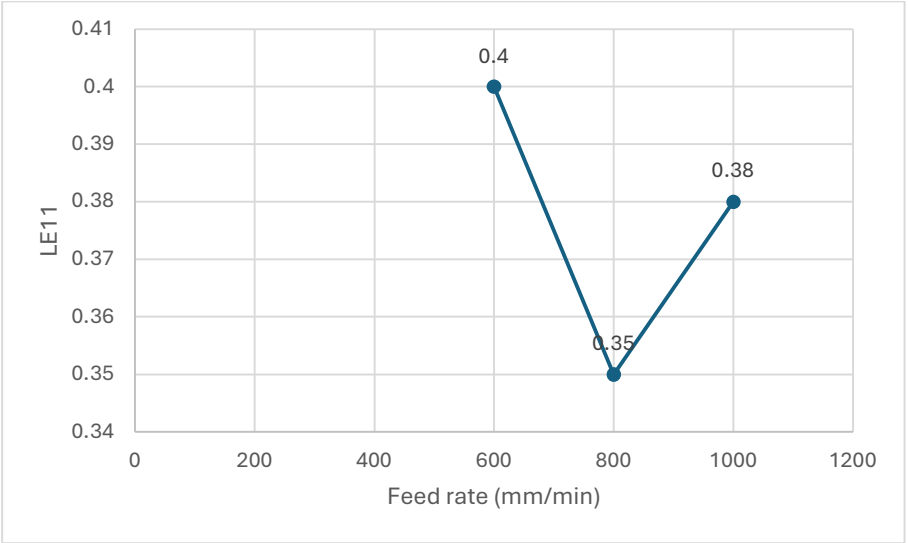

Fig 39: LE11 v/s feed rate plot

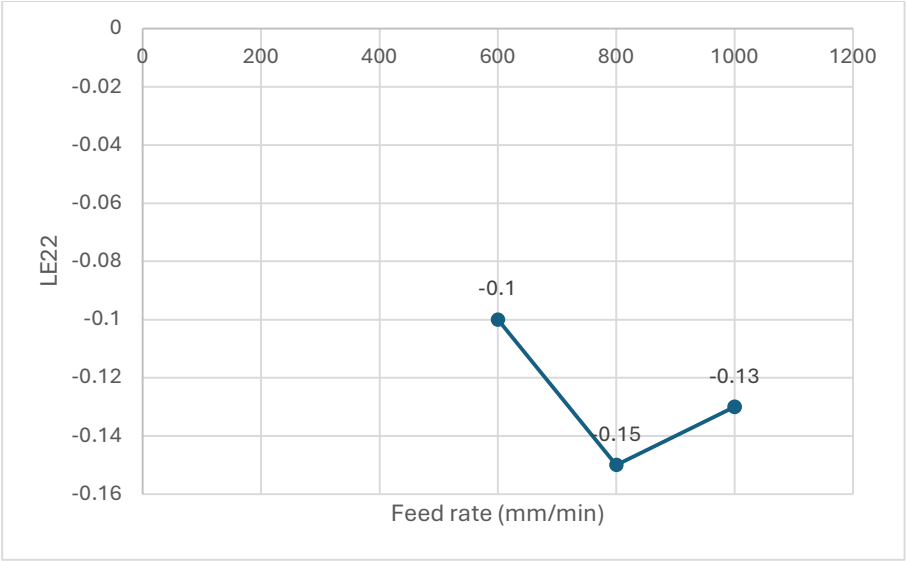

Fig 40: LE22 v/s feed rate plot

4.4.2 Upon changing step depth

The LE11 vs LE22 plots for step depths of 0.1 mm, 0.2 mm, and 0.3 mm show a similar deformation pattern, where LE11 increases in tension while LE22 becomes more negative due to compression during incremental forming. For the 0.1 mm step depth, the strain values extend up to approximately LE11 ≈ 0.40 and LE22 ≈ –0.13, indicating a wider strain range because the tool takes more incremental passes, allowing gradual but deeper stretching. At 0.2 mm, LE11 reaches around 0.35, while LE22 drops to roughly –0.11, showing moderately strong deformation with slightly reduced strain magnitude compared to 0.1 mm. For the 0.3 mm step depth, LE11 again rises toward 0.45, and LE22 reduces to around –0.10 to –0.11, but the slope appears smoother due to faster penetration per step. Overall, the comparison shows that smaller step depths (0.1 mm) generate the highest strain range because of more forming cycles, while larger step depths (0.3 mm) produce similar strain levels but in a shorter forming time, indicating more rapid material stretching.

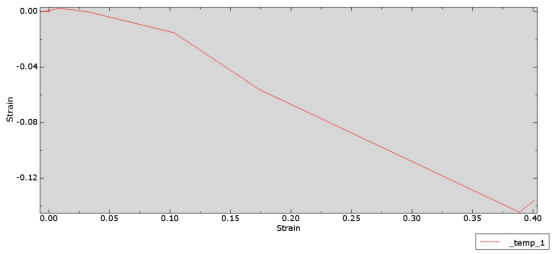

Fig 41: LE11 v/s LE22 plot (0.1 mm)

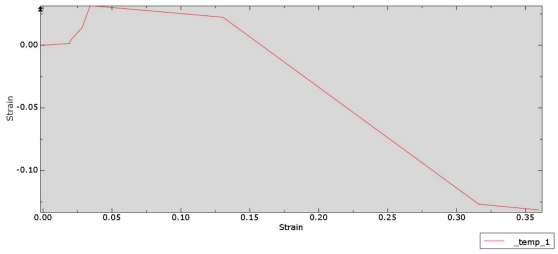

Fig 42: LE11 v/s LE22 plot (0.2 mm)

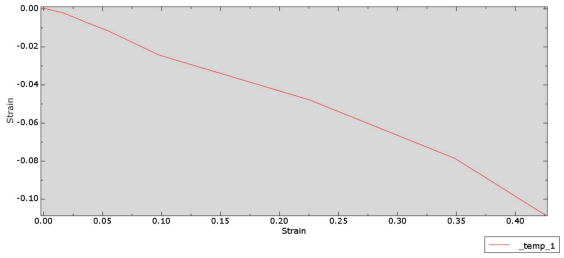

Fig 43: LE11 v/s LE22 plot (0.3 mm)

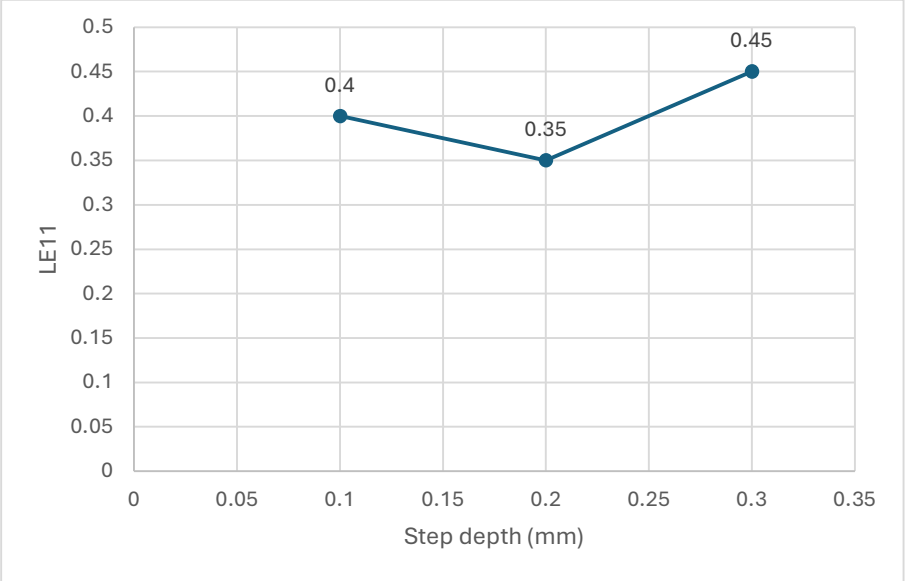

Fig 44: LE11 v/s step depth plot

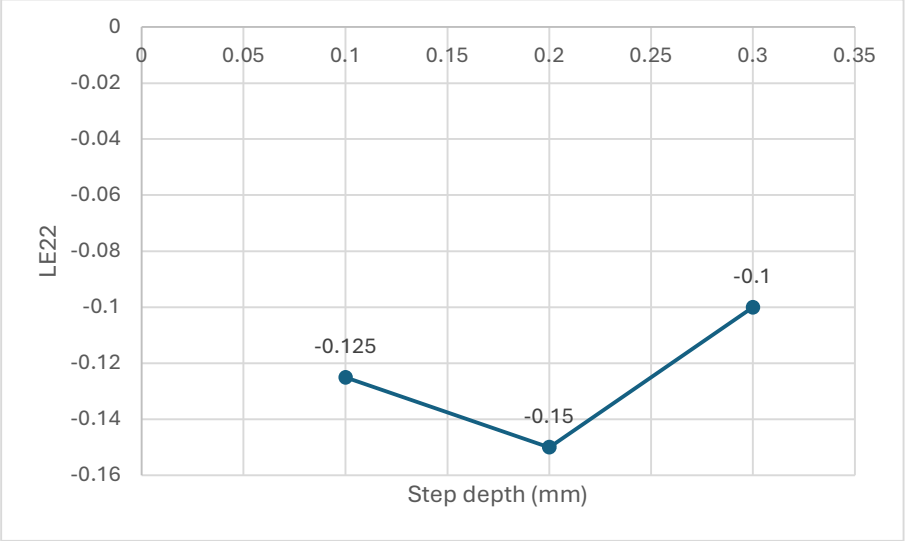

Fig 45: LE22 v/s step depth plot

4.4.3 Upon changing speed of tool (rpm)

The strain behaviour of the sheet changes noticeably with different tool rotational speeds. At 200 rpm, the sheet shows moderate stretching in the LE11 direction, reaching about 0.40, while the LE22 strain is around –0.08, indicating only slight thinning. At 300 rpm, the maximum LE11 value reduces to around 0.35, but the LE22 strain becomes more negative (–0.15), showing that the sheet undergoes more thinning and is therefore more likely to approach failure. At 400 rpm, the sheet displays the highest stretching in LE11 (0.60), while LE22

becomes positive (~0.10), which suggests that the thinning reduces and the material undergoes more uniform deformation due to increased heat and softening at higher rotational speed. Overall, 300 rpm is the most prone to failure, as it shows the highest thinning, whereas 400 rpm supports greater deformation without severe thinning.

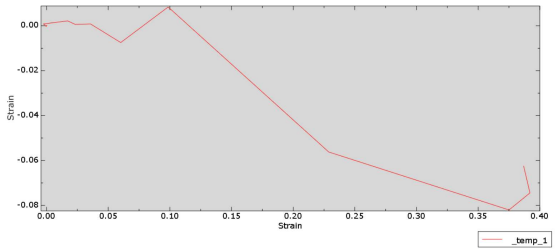

Fig 46: LE11 v/s LE22 plot (200 rpm)

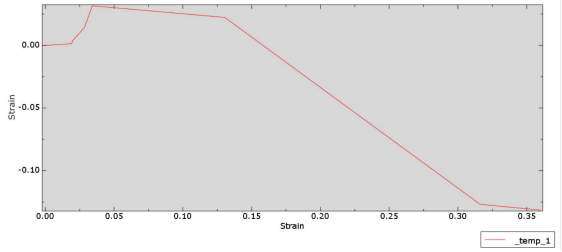

Fig 47: LE11 v/s LE22 plot (300 rpm)

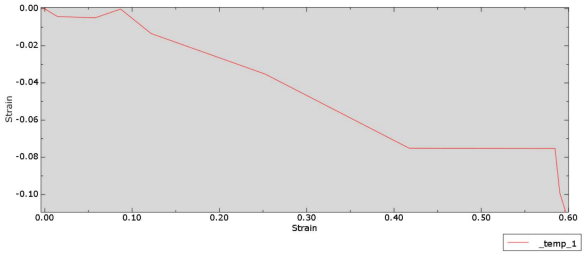

Fig 48: LE11 v/s LE22 plot (400 rpm)

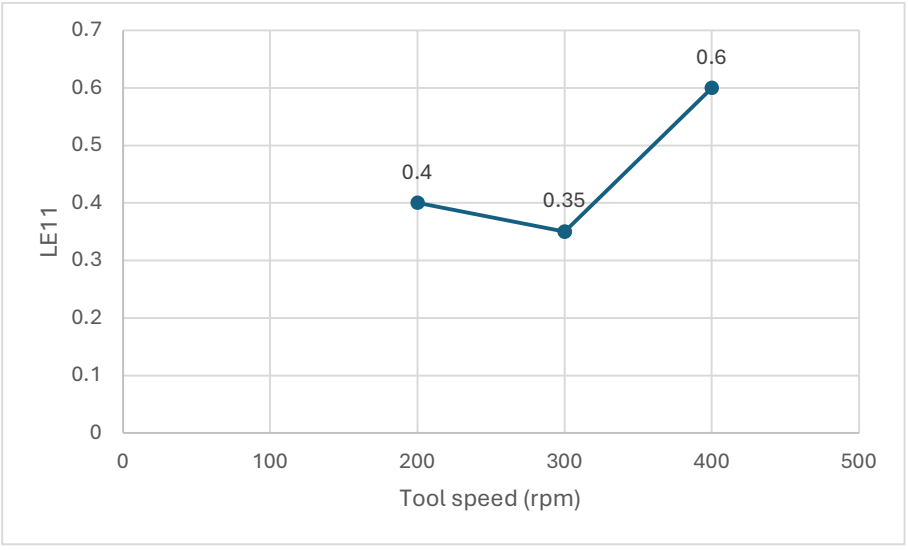

Fig 49: LE11 v/s tool speed plot

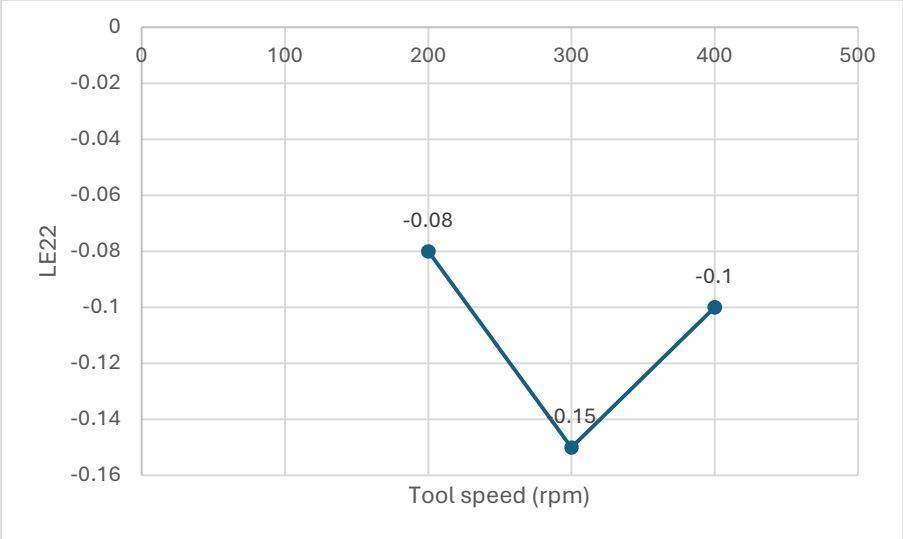

Fig 50: LE22 v/s tool speed plot

CHAPTER 5:
CONCLUSION AND FUTURE SCOPE

5.1 Validation and conclusion

The results of the present finite element simulation were compared with findings reported in two relevant research studies: “Influence of Process Parameters on Formability of Perforated Sheets in Single Point Incremental Forming” by Anees Jaleel and C. Sathiya Narayanan (2023), and “Finite Element Simulation and Experimental Analysis of Incremental Sheet Forming of Perforated Stainless Steel Sheets.” Both papers investigate process parameters such as spindle speed, feed rate, and step depth, and how these parameters influence deformation, stress distribution, strain evolution, and thickness behaviour in perforated stainless-steel sheets. A detailed comparison reveals that the behaviour observed in the present simulations aligns closely with the trends established in the literature, confirming the validity and reliability of the numerical model used in this work.

The first research paper highlights that spindle speed has a significant influence on both strain accumulation and forming stability. Extremely low speeds tend to increase contact time, resulting in higher localized stresses, while excessively high speeds can reduce deformation control due to rapid tool–sheet interaction. This observation matches the present results, where 300 rpm showed a more uniform strain distribution and lower peak von Mises stress compared to 200 rpm and 400 rpm, demonstrating that a moderate spindle speed offers a balanced forming condition. The literature also states that rotational speed influences frictional heat generation, which softens the material and affects the strain path. A similar trend is seen in the simulation, where 400 rpm allows higher stretching (LE11) without severe thinning due to increased material softening, again agreeing with the reported findings.

Both research papers further point out that feed rate affects the forming force and stress level by controlling the time the tool stays in contact with the sheet. Higher feed rates reduce the contact time and often lower the peak forces required for deformation. In the present study, although small variations in force were observed, the von Mises stress for 800 mm/min and 1000 mm/min remained lower or comparable to that at 600 mm/min, indicating smoother deformation and reduced stress concentration at higher feed rates. This supports the literature’s conclusion that increased feed rate improves forming efficiency without significantly increasing the risk of failure.

Step depth is identified in both papers as one of the most influential parameters affecting formability. Larger step depths accelerate deformation, increase thinning around perforations, and raise stress levels. The current simulation confirms this trend: 0.1 mm and 0.3 mm step depths produced higher peak stresses, while 0.2 mm resulted in the most stable deformation with a more uniform stress distribution. This aligns with the experimental findings that moderate step depths reduce localized overstressing and improve thickness uniformity. Additionally, both research papers report that perforated sheets naturally experience stress concentration near hole edges, and the same behaviour is clearly captured in the present von Mises stress contours, showing accurate representation of real forming behaviour.

Overall, the comparison with published research confirms that the simulated deformation patterns, stress concentration zones, strain responses, and thickness changes closely match experimental and numerical results reported in literature. This strong agreement validates the modelling approach, material definition, boundary conditions, and mesh strategy used in this study. Based on the results, it can be concluded that process parameters must be carefully selected to optimize forming quality, especially for perforated sheets which are more susceptible to localized deformation. Among all parameter combinations tested, 300 rpm spindle speed, 800 mm/min feed rate, and 0.2 mm step depth consistently provided the most balanced performance with controlled thinning, moderate stresses, and favourable strain behaviour. The validated outcomes of this study provide a reliable foundation for future experimental investigation and contribute to the understanding of forming behaviour in perforated SS304L sheets.

5.2 Future Scope

- The simulation work can be extended to experimental validation using the same process parameters to verify thinning, contact force and strain trends.
- Different perforation patterns and hole sizes can be studied to analyse their effect on formability and stress concentration.
- Thermally assisted ISF (warm or laser-assisted forming) can be explored to reduce thinning and improve ductility in perforated sheets.
- The study can be expanded by comparing different biocompatible materials, such as titanium and aluminium alloys, for medical applications.
- Toolpath optimisation techniques can be investigated to minimize local stresses and obtain better final dimensional accuracy.

- Failure prediction or damage modelling can be incorporated to identify conditions leading to cracking around perforations.

REFERENCES

- A. Chennakesava Reddy, Experimental and Numerical Studies on Formability of Stainless Steel 304 in Incremental sheet Metal Forming of Elliptical cups, International Journal of Scientific & Engineering Research, Volume 8, Issue 1, January-2017, ISSN 2229-5518
- Ajay Kumar, Vishal Gulati, Parveen Kumar, Hari Singh, Vinay Singh, Sanjay Kumar, Abid Haleem, Parametric Investigation of Forming Forces in Single Point Incremental Forming, Materials Today: Proceedings 24 (2020) 644-617
- Anees Jaleel, C. Sathiya Narayanan, Formability investigation of perforated austenitic SS 304L sheets using SPIF, Journal of Manufacturing Processes 104 (2023) 44–58
- Anees Jaleel, C. Sathiya Narayanan, Optimization, finite element simulation, fractography and tool wear analysis during SPIF process of perforated stainless steel sheets, Materials Today Communications 36 (2023) 106823
- Antonio Piccininni, Francesco Gagliardi, Pasquale Guglielmi, Luigi De Napoli, Giuseppina Ambrogio, Donato Sorgente, Gianfranco Palumbo, Biomedical Titanium alloy prostheses manufacturing by means of Superplastic and Incremental Forming Process, MATEC Web of Conferences 80, 15007 (2016)
- C. Veera ajay, Parameter Optimization in Incremental Forming of Titanium Alloy Material, Trans Indian Inst Met (2020) 73(9):2403-2413
- E. H. Uheida, G. A. Oosthuizen, D. Dimitrov, Investigating the Impact of Velocity on the Process Conditions in Incremental Forming of Titanium sheets, Procedia Manufacturing 7 (2017) 345-350
- Elizabeth M. Mamros, Fabian Maa, A. Erman Tekkaya, Brad L. Kinsey, Jinjin Ha, Martensitic transformation of SS304 truncated square pyramid manufactured by Single Point, Incremental forming, CIRP Journal of Manufacturing Science and Technology 55 (2024) 28-41
- Elizabeth M. Mamros, Lauren E. Blaha, and Christian A. Kauffman, Investigation using single point incremental forming (SPIF) to fabricate patient-specific, titanium orbital floor implants
- Gabriel Centeno, Andres Jesus Martinez-Donaire, Isabel Bagudanch, Domingo Morales-Palma, Maria Luisa Garcia-Romeu and Carpoforo Vallellano, Revisiting Formability and Failure of AISI 304 sheets in SPIF: Experimental Approach and Numerical Validation, Materials 2017, 7, 531

- Hui Zhu, Hengan Ou, Analytical modelling of local contact behavior in incremental sheet forming, Journal of Materials Research and Technology 36 (2025) 6741-6757
- Manish Oraon, Soumen Mandal, Vinay Sharma, Investigation into the process parameter of single point incremental forming (SPIF), Materials Today: Proceedings 33 (2020) 5218-5221
- Rahul R. Gurpude, Amrut Mulay, Pawan Sharma, Formability improvement in die less forming process of Ti Gr. 2 perforated sheet: experiment method and finite element analysis, International Journal on Interactive Design and Manufacturing (UIDeM) (2025) 19:3633-3645
- Ruxiong Li & Tao Wang, Research on Single Point Incremental Forming Characteristics of Perforated TA1 Sheet, Metals 2022, 12, 1944
- Saurabh Thakur, Sant Ram Chauhan, Patient-Specific Cranial Implant Fabrication: Evaluating Single-Point Incremental Forming with Perforated Titanium Grade-2 Sheets, JMEPEG (2015) 34:7113-7123.
- Seyyed Emad Seyyedi, Hamid Gorji, Mohammad Bakhshi-Jooybari, Mohammad Javed Mirnia, Comparison between conventional press-working and incremental forming in hole flanging of AA6061-T6 sheets using a ductile fracture model, International Journal of Solids and Structures 270 (2023) 112225
- Valentin Oleksik, Tomasz Trzepiecinski, Marcin Szpunar, Lukasz Chodola, Daniel Ficek and Ireneusz Szczesny, Single-Point Incremental Forming of Titanium and Titanium Alloy Sheets, Materials 2021, 14, 6372
- https://www.researchgate.net/figure/The-basic-principle-of-ISF-and-forming-process-a-to-b_fig1_344446558
- https://share.google/images/hqwMWXUGmQ3GU0P1q